Active2012

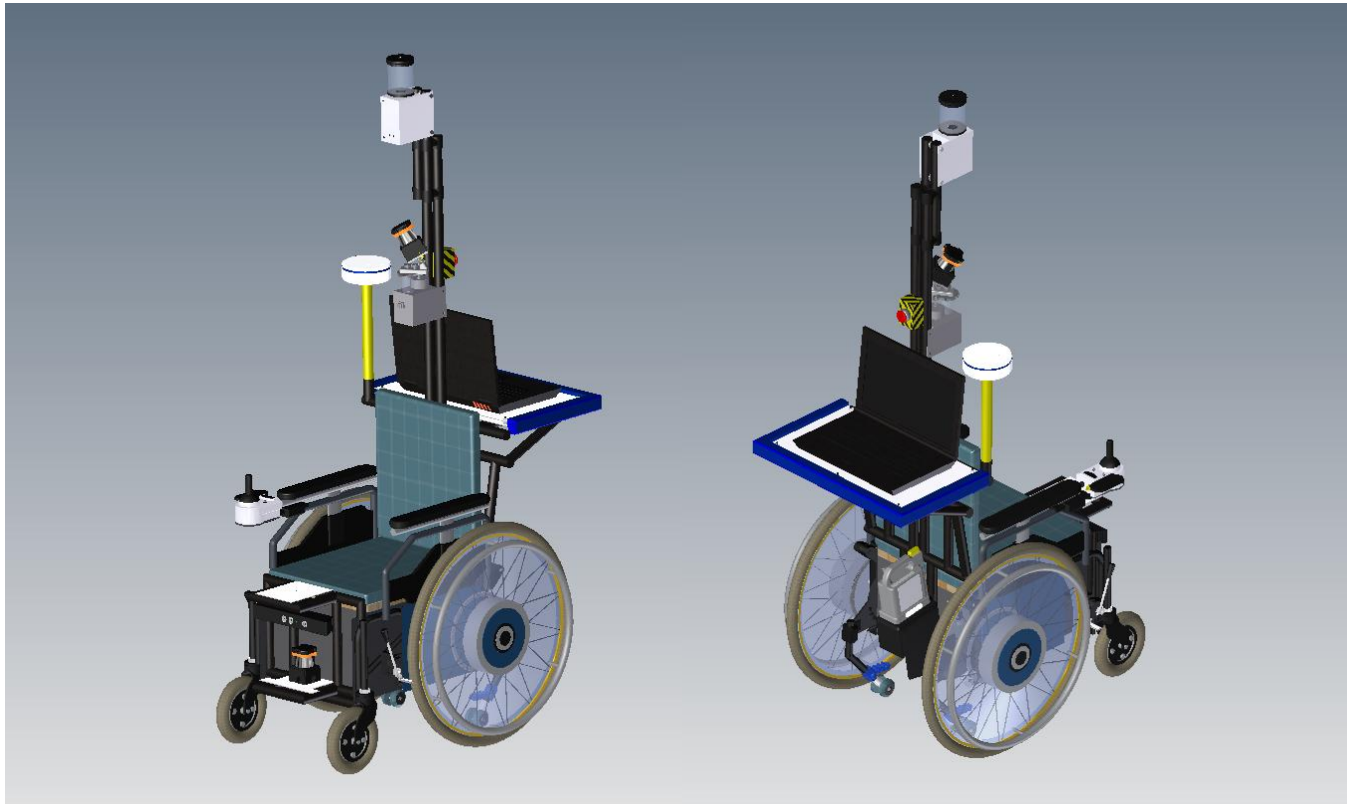## HOSEI UNIVERSITY

Faculty of Science and Engineering, Hosei University 3-7-2 Kajinocho Koganei, Tokyo 194-8584, Japan

E-mail; ikko@hosei.ac.jp

Faculty Advisor Statement

I hereby certify that the engineering design on Active2012 was done by the current student team and has been significant and equivalent to what might be awarded credit in a senior design course.

Signed *Kazuyuki Kobayashi*   Date *April 28. 2012*

Prof. Kazuyuki Kobayashi   **April 28, 2012**

Prof. Kajiro Watanabe

Prof. Kaoru Suzuki

Prof. Kazuyuki Kobayashi

1. Introduction

Hosei University's IGVC team consists of members of the autonomous robot team (ARL), which is an undergraduate and graduate student-led robotics research group. Since 1996, our team has been building upon ARL's experience in robotics competitions such as the 2011 Intelligent Ground Vehicle Competition (IGVC). In the IGVC 2011, we were placed 3rd overall, and 5th, 2nd, and 1st in the Navigation, Autonomous, and JAUS challenges, respectively. Building upon previous successes, Active2012 has been redesigned to address a new Auto-Nav challenge under the IGVC 2012 rules, with higher intelligence and innovative features.
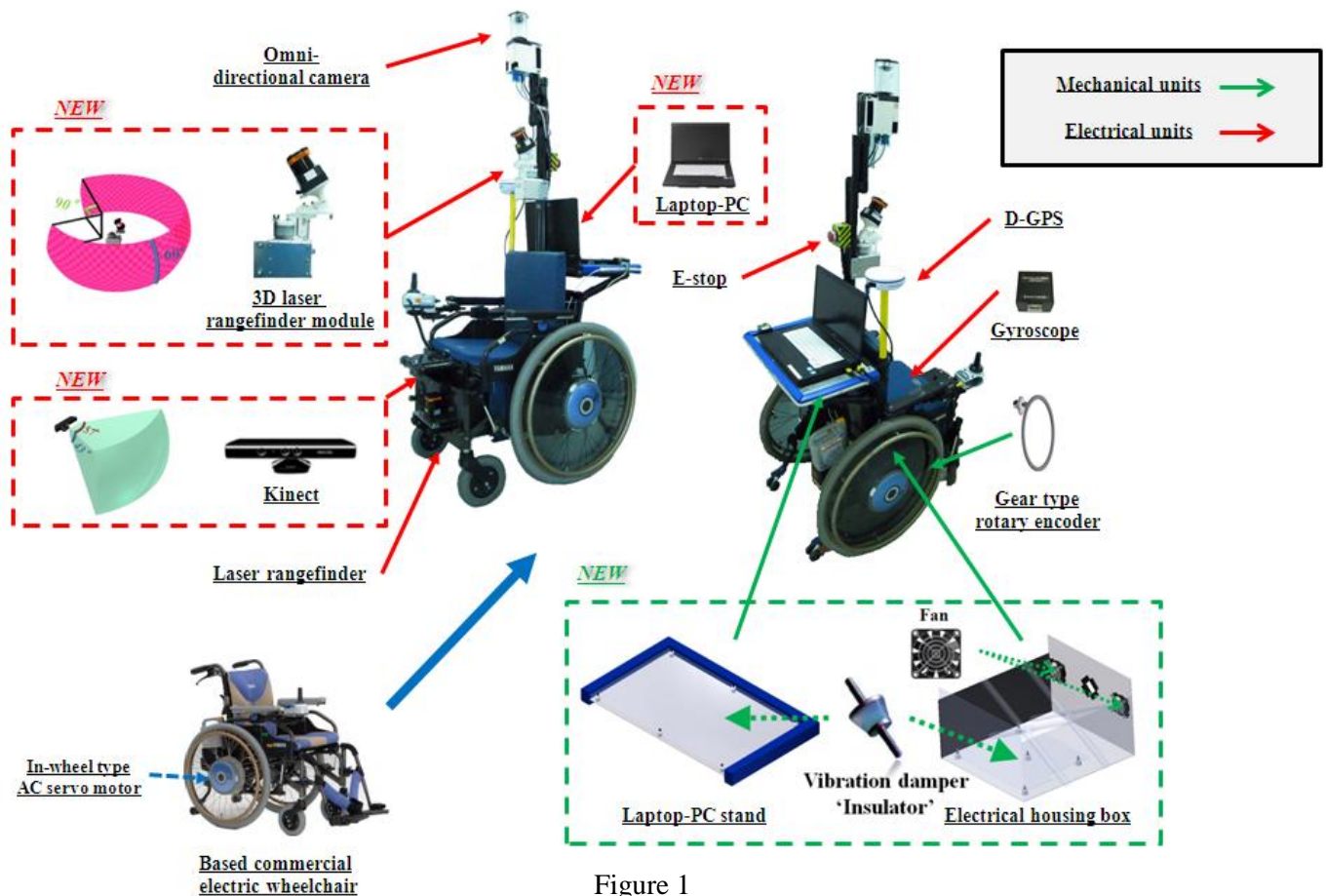
2. Effective Innovation

Figure 1

Active2012 is based on Active2011's chassis and includes new hardware, software, and multiple noteworthy innovations to adhere to the rules of the new Auto-Nav challenge as shown in Figure 1. In order to redesign Active2012, we introduced a new failure mode and effect analysis -based design approach. Application of this approach can help in summarizing solutions to identified problems as follows:
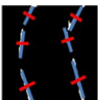
Table 1 Hardware problems & solutions

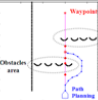| Problem	Solution	
The laser rangefinder cannot identify the shape of the obstacles.	We developed a **3D laser rangefinder module** that is rotated by a unique swinging mechanism, to identify the shape of three-dimensional obstacles.	
Unknown sensor errors induce vibration problems, particularly when the vehicle runs over irregular terrain.	We use a new **vibration insulator** to suppress vibration in the electrical housing box and the laptop-PC.	
Exposure to direct sunlight and problems in the heater power circuit cause overheating in the electrical housing box.	We embedded two **electrical fans** in the electrical housing box to prevent its overheating.	

Table 2 Software problems & solutions

Problem	Solution	
Limitation of maximum speed because of the environment recognition processing time.	We introduced a new lane detection algorithm that is **based on the use of eigenvectors** instead of the Hough transform.	
	In order to reduce processing time, **pruning algorithm is implemented in our A* algorithm** (for path planning).	

3. Team Organization & Design Process

3.1 Team Organization

Figure 2 shows the organization of our team, which is composed of eleven members: six undergraduate and five graduate students. Team members were grouped into hardware, software, and electrical teams according to their area of expertise. We selected a student team leader to supervise the teams and all their projects.

The mechanical team is responsible for all physical aspects of the vehicle, including design and fabrication. The electrical team is responsible for sensor selection, electronics, electrical wiring, and computer hardware. The software team is responsible for algorithm design and programming implementation. Overall, over 1200 person-hours have been spent

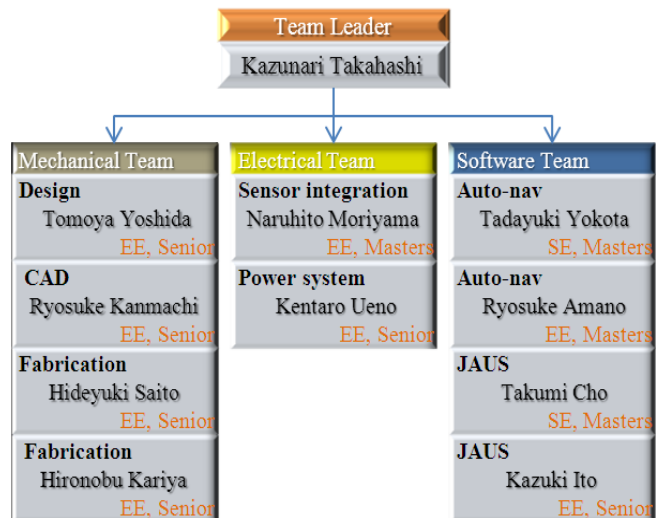this year working on Active2012 and its specific software improvements.

Figure 2 Team Organization

3.2 FMEA Design Process

In last year's competition, awkward sensor errors had occurred, especially when the vehicle was running at high speed in both the autonomous and the navigation challenges. In order to identify this problem, we employed a new design and analysis process called a failure mode and effect analysis (FMEA). FMEA is a methodology for analyzing potential reliability problems early in the development cycle, where it is easier to take actions to overcome these issues, thereby enhancing reliability through design.

Figure 3 FMEA design process
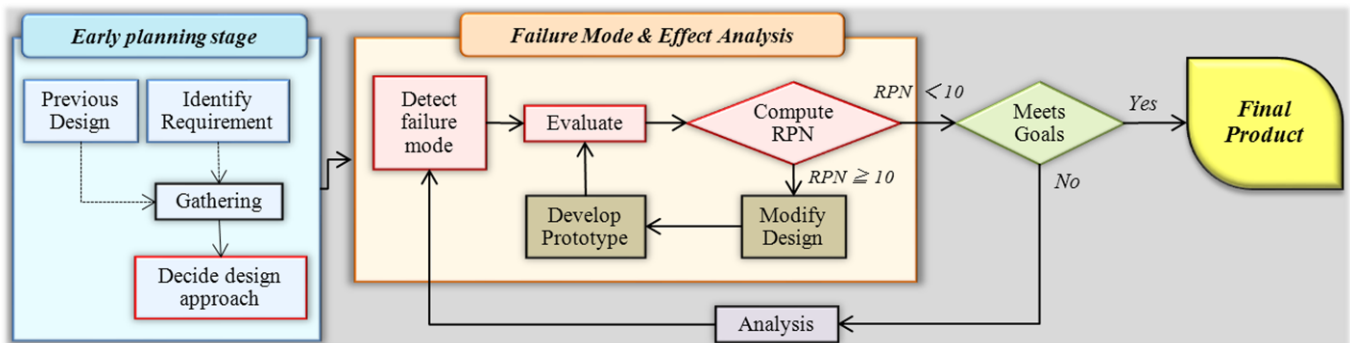
Depending on the importance of the errors, they are ranked according to three parameters (severity, occurrence, and detection) on a four-point scale (1: low risk; 2: permissible range; 3: must improve; 4: measures essential). According to these error scales, the risk priority number (RPN) for the necessity of improvement can be calculated by the following equation:

RPN = Severity * Occurrence * Detection

The RPN values range from 1 (absolute best) to 64 (absolute worst). If the RPN value is greater than 10, we have to consider essential improvements. Table 3 presents our actual FMEA table for Active2012 design improvements.

Table 3 FMEA table

No	Item	Function	Failure mode	Cause of failure	Causes				Improvement strategy	Results			
					SEV	OCC	DET	RPN		SEV	OCC	DET	RPN
1	Electrical housing box	Circuits protect	Heat	Unknown sensor error	3	3	3	27	Equipped with two fans	2	2	2	8
2			Vibration		4	3	4	48	Employed vibration inheritor	1	1	2	2
3	PC	Processor		Failure of the HDD	3	2	4	24		1	1	2	2
4	Laser rangefinder	Obstacle detection	Dead angle	Collision with the obstacle	3	3	2	18	Developed 3D LRF module	1	1	1	1
5	Rubber encoder rubber	Angle detection	Rubber degradation	Cause the measuring error	2	3	3	18	Changed the gear type rotary encoder	1	2	1	2

4. Electrical Design
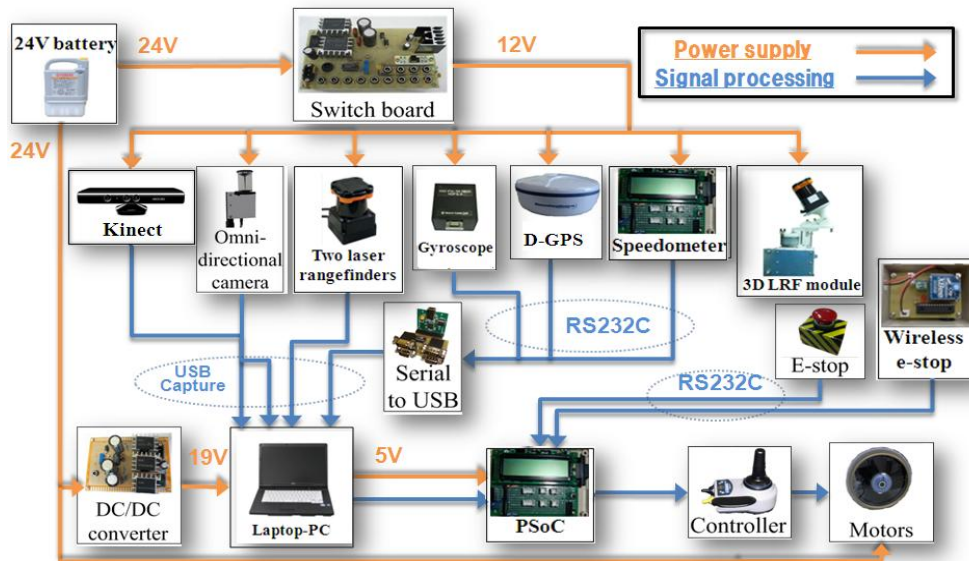
4.1 Power System and Sensor Integration

Figure 4 Sensor & integration

A 24 V 6.7 Ah 5 h battery is used in Active2012. This battery supplies all motor actuators, the laptop-PC, and sensors (laser rangefinder, D-GPS, gyroscope, omni-directional camera, Kinect, 3D laser rangefinder module). Figure 4 shows the developed power supply system. Environmental information is acquired from sensors that are integrated in and evaluated by the laptop-PC. The processing result of the laptop-PC is sent through an RS232 interface to the PSoC microcontroller, and from there to the vehicle controller. Figure 4 shows the connectivity and integration of the sensor signals and power supply lines. All sensors and critical electronic equipment are protected by breakers and fuses throughout the power supply system. The power supply jack has been designed to prevent erroneous voltage connections.

4.1.1 Safety

In order that it follows the imposed safety regulations, Active2012 is equipped with two different types of emergency stop systems (E-Stop and wireless E-Stop) and a safety light. The manual E-stop button is red, while the E-stop box has black and yellow stripes. The wireless E-stop is designed on the basis of a wireless communication module through the PSoC microcontroller, using an XBee transmitter/receiver. In order to synchronize the manual and navigation modes, we installed a helically wrapped LED ribbon strip on the central pole of the vehicle, as safety light. The LED ribbon displays a stable (turned on) or flashing light when the vehicle is in the autonomous or manual mode, respectively. According to the specifications of the XBee device, the maximum wireless communication range is about 33 meters, allowing the vehicle to be stopped remotely in case of an emergency.

4.2 Computer

In order to ensure a memory large enough for map memorization in the Auto-Nav challenge and expand the number of USB ports for new sensors, we selected a new laptop-PC with 4GB RAM and 6 USB ports. Table 4 lists specification differences between last year's and this year's laptop-PC.

All sensor information is transmitted through USB cables.

Table 4 Laptop-PC change

	previous	New
Laptop PC	ASUS U33JC	FUJITSU LIFEBOOK A561/C
Memory	2GB	4GB
USB port	USB2.0 × 2 USB3.0 × 1	USB2.0 × 4
CPU	2.53-GHz Intel core i5 processor	2.60-GHz Intel core i5 processor

4.3 Sensor

Table 5 presents the specifications of the sensor suite. Active2012 uses seven types of sensors to perceive the surrounding environment. Specifically, it uses laser rangefinder (LRF), 3D laser rangefinder module (3D LRF module), Kinect, omni-directional camera, D-GPS, optical fiber gyroscope and speedometer to perceive the environment and support intelligent operations.

Table 5 Sensor suite

Sensor	Role	Description
Laser rangefinder	Obstacle detection All obstacles	HOKUYO UTM-30LX **Feature:** Detect obstacles ・Scan rate: 0.4 seconds ・Angular resolution: 0.25 degree
3D Laser rangefinder module	Obstacle detection All obstacles	HOKUYO UTM-30LX with roundly swinging mechanism **Feature:** Identify three-dimensional obstacle shapes ・Flat view: 270 degree, vertical view: 60 degree ・Scan rate in 1 field: 0.8 seconds
Kinect	Obstacle detection Flags	Microsoft Kinect **Feature**: Equipped with RGB camera and depth sensor ・Flat view: 57 degree, vertical view: 43 degree ・Image resolution provided: 640×480
Omni-directional camera	Lane detection Obstacle detection Holes	SONY CCD EVI-370 with Hyperbolic mirror **Feature**: Acquires360 degree image ・Image resolution provided: 640×380
D-GPS	Pose detection	Hemisphere A100 **Feature**: Provides latitude and longitude information ・Update Rate: Up to 20 Hz position with 95% ・Horizontal Accuracy: 0.6 meters (GPS mode)
Optical fifer gyroscope	Angle detection	HITACHI HOFG-3 **Feature**: Detects the relative orientation of the vehicle ・Angular speed: Up to 100 degree per second
Speedometer	Speed detection	We are designed speedometer using PSoC microcontroller **Feature**: Converts the rotation angles obtained by rotary encoder to speedometer data

New sensors (1) Kinect and (2) 3D LRF module are described below.

(1) Kinect

An omni-directional camera may not have enough resolution for recognizing a color flag according to the new Auto-Nav challenge rules, because the area of the flag is too small. In order to recognize color flags robustly, we incorporated Kinect, which is equipped with an RGB camera and a depth sensor, to recognize both the shape and the color of the flag simultaneously with a sufficient resolution of 640×480 pixels.
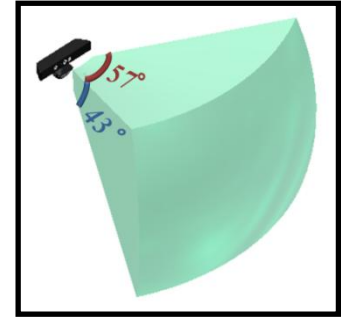

Figure 5 Area detectable by Kinect

(2) 3D laser rangefinder module

Because the rules allow map memorization, we employ two LRF detect both obstacles. One LRF sets the horizontal angle to the ground, which is mainly used to detect obstacles as landmarks for map memorization. The other prevents dead angles of the first LRF, especially near both sides of the vehicle. We developed a new 3D LRF module, depicted in Figure 6. This module is composed of an LRF unit equipped with a roundly swinging mechanism. The horizontal and vertical view angles of the developed module are of 270° and about 60°, respectively.
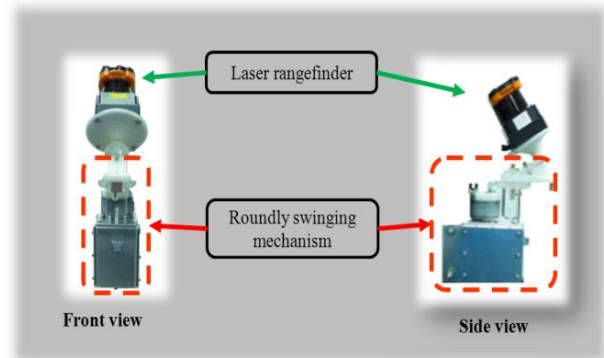
Figure 6 Developed 3D laser rangefinder module

Figure 7 shows the change in direction of the LRF by the roundly swinging mechanism. One LRF is fixed on the two-dimensional free gimbal mechanism that rotates the inclined axis around the main body of the sensor module. The rotation part is driven by the DC motor. The front of the LRF is kept almost in a constant direction even though it is driven rotationally, being moved only vertically by the swinging motion; the cable is never twisted. Figure 8 shows the 3D detection area of our proposed 3D LRF module.

Figure 7 Change in direction of the LRF

Figure 8 Three-dimensional detection area

6

Figure 9 shows a schematic block diagram for the proposed 3D LRF module control. The rounding speed is controlled by using a DC motor with a rotary encoder. The origin of the LRF direction is determined by the initial angle position that is detected for each scanning cycle by a photo-interrupter switch.

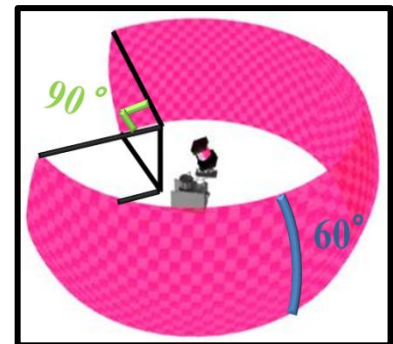Based on the rounding speed and detection of the initial position, we can identify the LRF's direction and orientation. PSoC microcontroller is used for regulating the rotation speed and detection of the initial angle position. The 3D LRF module can acquire environmental information around the vehicle at a rate of 0.8 seconds per scanning cycle.
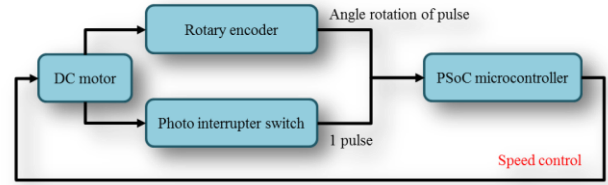

Figure 9 Rotation at uniform rate for each scanning

4.3.2 Detection area

According to the new Auto-Nav Challenge rules, Active2012 has to recognize obstacles such as barrels, barriers, fences, flags, and other complex obstacles. In order to distinguish these obstacles, we use the LRF, 3D LRF module, the omni-directional camera, and Kinect. Figure 10 shows the detection areas of all sensors. The role of these four sensors is summarized in Table 6.

Table 6 Role of the sensors

| Sensor	Role
Laser rangefinder	Detection of distant obstacles up to 30 m for SLAM navigation.
3D laser rangefinder module	Near detection of three-dimensional shape obstacles up to 10 m.
Kinect	The combination of an RGB camera with a depth-image sensor allows detecting and identifying color flags (red or blue) within a distance of 2 m.
Omni-directional camera	Mainly used for the detection of stable lanes and obstacles within a radius of 3 m.
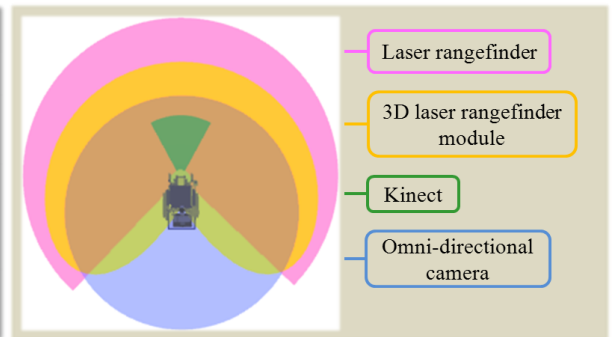
Figure 10 Detection areas of all sensors

Dead ends and traps can be recognized by using a navigation map that is generated by long-range sensors. Active2012 recognizes dead ends and/or traps according to a generated navigation map. In such a scenario, Active2012 executes a zero-radius turn to go back and find the correct navigation course.

5. Mechanical Design

In order to prevent awkward unstable sensor errors that occurred in last year's Active2011, we have now included FMEA, whose details are described in section 3.2. Following the FMEA to prevent unstable sensor errors, we analyzed the problems encountered in Active2012 and decided on the mechanical design concept: **industrial-strength quakeproof aware vehicle.** Figure 11 shows the Active2012 model that we designed by using Autodesk Inventor Professional 2011.
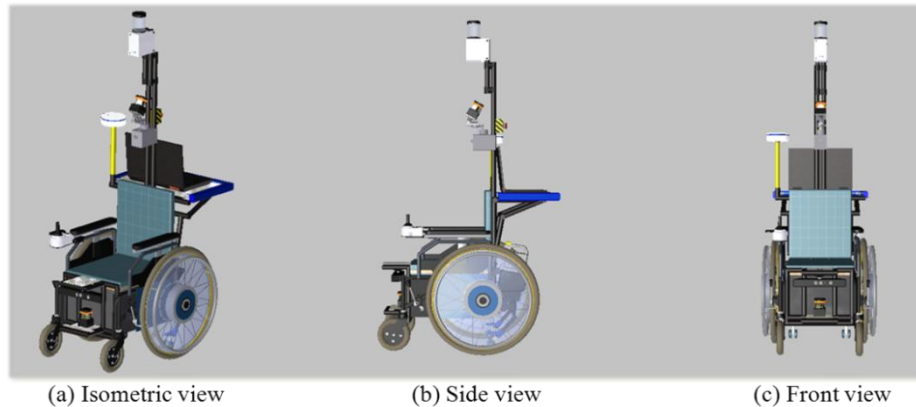

(a) Isometric view   (b) Side view   (c) Front view

Figure 11 Active2012 CAD

As depicted in Figure 11, Active2012 mainly consists of three parts:

(1) To enhance reliability, we are using the base chassis and actuator of a commercial electric wheelchair.

(2) For space efficiency in the chassis, we designed a new electrical housing box.

(3) We relocated sensor units based on the FMEA results.

5.1 Chassis

The base vehicle shown in Figure 12 is the YAMAHA electric wheelchair (JW-Active), which has in-wheel motors, thus eliminating the additional reduction gearbox and resulting in a simple frame and lightweight configuration of the base chassis. Using this commercially available electric wheelchair as the base guarantees chassis reliability and considerably reduces the mechanical manufacturing time.

Figure 12 JW-Active

5.2 Actuator

The actuators that drive the vehicle are two 24-V AC direct-drive servomotors that are originally mounted on the left and right sides of the 24-in wheels. The use of direct-drive motors enables a free vehicle frame design in comparison to regular speed reducer drive motor designs.

Figure 13 In-wheel motor

5.3 Rotary encoder

For precise local motion estimates, including individual wheel speed, Active2012 uses a rotary encoder mounted on each wheel axle. Last year, the rubber rotary encoder frequently caused speed errors because of rubber degradation caused by slips between the rotary encoder and the wheel axle. To prevent rotational slip, we developed a new gear type rotary encoder, as shown in Figure 14. Because of gear accuracy requirements, both the gear type rotary encoder and the wheel axle gear were manufactured using a compact milling machine (MDX-20).
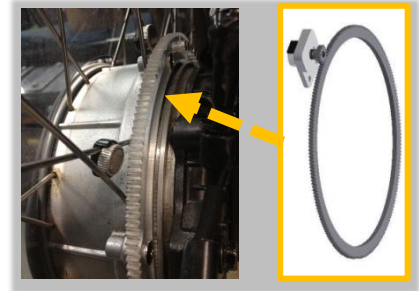

Figure 14 Gear type rotary encoder

The designed gear has a ratio of about 1:7 and is made of acrylic board.

5.4 Durability

We summarize the application of the FMEA method to two problems, vibration and heating, to enhance our vehicle durability.
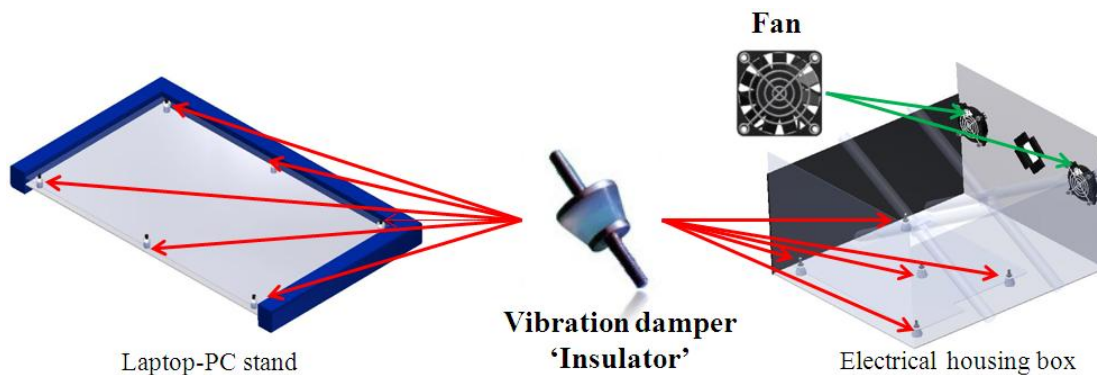

Figure 15 Applied vibration insulator

(1) Vibration problem

During the competition of IGVC2011, awkward unknown sensor errors had occurred, especially when the vehicle was running over rough terrain. Because of the original chassis, our vehicle is driven by an in-wheel motor that does not have an anti-vibration damper. Ground vibrations directly affect the chassis, causing unpredictable signal disconnections between the electrical housing box and the laptop-PC. This year, in order to avoid the vibration problem, which is a primary cause of sensor errors, we introduced a new vibration damper "insulator" to support both the laptop-PC and the electrical housing box on the chassis.

Figure 15 shows the vibration damper that we used. Alpha GEL vibration dampers effectively damp micro vibrations or light load vibrations in particular, which cannot be eliminated by conventional dampers such as rubber. They also provide long-term sustainability and perform well under demanding environments. Depending on the weight of the laptop-PC and the electrical housing box, we use five and six insulators for the electrical housing box and the laptop-PC stand, respectively.

(2) Heating problem

Figure 15 shows the fan that we used. Depending on the weather conditions during the competition day, the heating problem has to be taken into account as a key factor. The electrical housing box is one of the primary elements to be protected from heating. Heating problems in the electrical housing box are caused by direct sunlight exposure and problems in the heater power circuit. To prevent overheating of the electrical housing box, we embedded two electrical fans in the box that would transfer heat to the outside.

5.6 Cost

The costs involved in developing Active2012 are summarized in Table 7.

Table 7 Estimated development costs for Active2012

Components	Retail Cost	Team Cost	Description
YAMAHA JW-Active	$5,600	$0	Electric wheelchair
HITACHI HOFG-3	$5,800	$0	Optical fiber gyroscope
HOKUYO UTM-30LX ×2	$8,000	$0	Laser range finder
SONY EVI-370	$360	$0	CCD camera
Hyperbolic mirror	$4,600	$0	
Hemisphere A100	$2,414	$0	D-GPS
Microsoft Xbox360 Kinect	$150	$150	3D range image camera
I-O DATA GV-USB2	$50	$50	USB video capture cable
FUJITSU LIFEBOOK A561/C	$1,000	$1,000	Laptop-PC
Mechanical parts	$536	$536	Various mechanical components
Electronic parts	$158	$158	Various electrical components
Total	$28,668	$1,894	

6. Software

6.1 Software Design

Because of regulation changes regarding maximum speed, we have to reduce the processing time of the vehicle speed control system to achieve the maximum speed of Active2012.

To reduce the processing time, we improved the speed of the lane detection (Section 6.3) and path planning (Section 6.4) algorithms. Significant changes were made in eigenvector-based algorithms and path planning by using extended A*.

6.2 Mapping

In IGVC2010, the vehicle could not run through the obstacle area in the autonomous challenge course because of the limited viewing angle of the laser rangefinder. To address this problem, we used an additional laser rangefinder to enhance the viewing angle and thus be able to detect obstacles effectively.

Because we are allowed to use map memorization in IGVC2012, we have applied the simultaneous localization and mapping (SLAM) algorithm for position estimation in Active2012. Figure 16 (a) shows an environmental information map acquired by the LRF. IGVC obstacles tend to be cylindrical and to have a constant radius. Therefore, we apply a circular Hough transform to detect obstacles as constant-radius circles. Figures 16 (b) and (c) show estimated constant-radius-circle positions by applying the circular Hough transform, and the reconstructed obstacles including the hidden shape, respectively.

(a) Information acquired by the LRF   (b) Application of the Hough transform   (c) Correct prediction of the obstacles
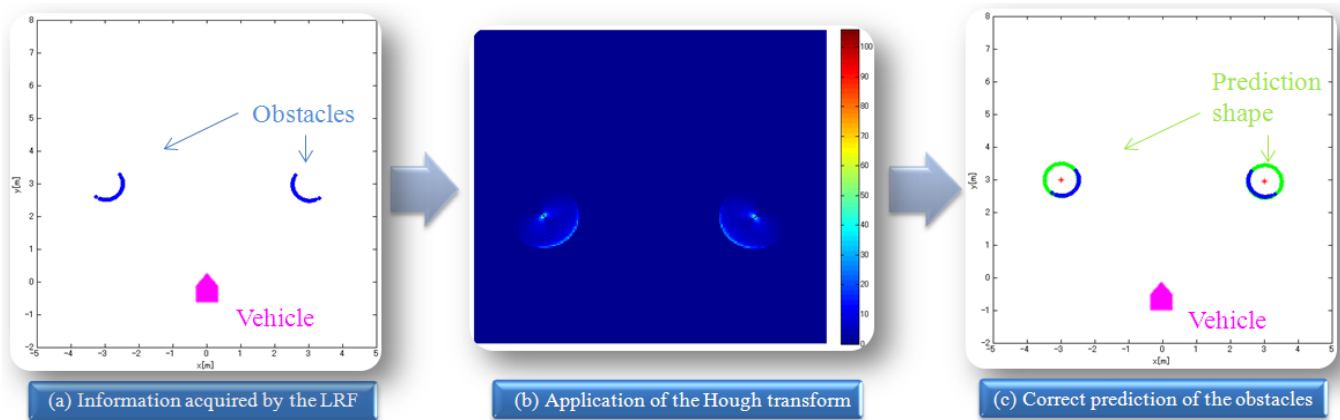
Figure 16 Mapping

6.3 Lane Detection

During IGVC2011, we were confident about the reliability of the lane detection algorithm that was based on omni-directional images. The developed lane detection algorithm was robust and stable enough to detect lanes correctly. However, time calculation was a problem; the vehicle could not complete the task within the required time in the autonomous challenge. In order to solve the problem of a large image processing time, we profiled the lane detection algorithm to identify the most time-consuming part. Table 8 shows a comparison of processing times between the conventional and optimized algorithms. The optimized algorithm improved the processing speed by about 1.5 times.

Table 8 Comparison between conventional and optimized algorithms

Profile Summary
Generated 02-Apr-2012 16:44:00 using cpu time.

Function Name		Calls	Total Time	Self Time*	Total Time Plot (dark band = self time)
lane fit	←Last year's	8	0.062 s	0.062 s	▬
eig lane	←This year's	8	0.046 s	0.046 s	▬

Figure 17 (a) to (g) shows the basic procedure of image processing. Figure 17(a) shows an image captured by the omni-directional camera. Figure 17(b) shows the reconstructed ground image. After reconstruction, the RGB color image is converted to a grayscale image using only the B component. Figure 17(c) shows the grayscale image. By using a referenced lane template image prepared in advance, normalized template matching is applied to detect the lanes. This technique is robust to noise and sensitive to lanes. The template-matched image is converted to a binary image by comparing the thresholds. Figure 17(d) shows the binary image. The isolated noise in the binary image is removed by the combined algorithms of the labeling and morphological thinning processes; this is called logical filtering. Figure 17(e) shows the logically filtered image. Figure 17(f) shows a typical example of the region-segmented results. The quadtree decomposition method is used to distinguish both lane areas and other areas. Figure 17(g) shows the lane enhancement results. Lane enhancement is achieved based on the labeling results for removing small isolated areas.

On the basis of differences between last and this year's algorithms, we now use eigenvectors instead of RANSAC (RANdom SAmple Consensus) for straight-line approximation. The eigenvector-based straight-line approximation is able to detect major and minor axes of the lane as shown in Figure 17 (h). Replacing RANSAC with the calculation of eigenvectors and eigenvalues, we estimate major and minor axes to identify the shape of the lane, hence resulting in faster and more precise lane detection.
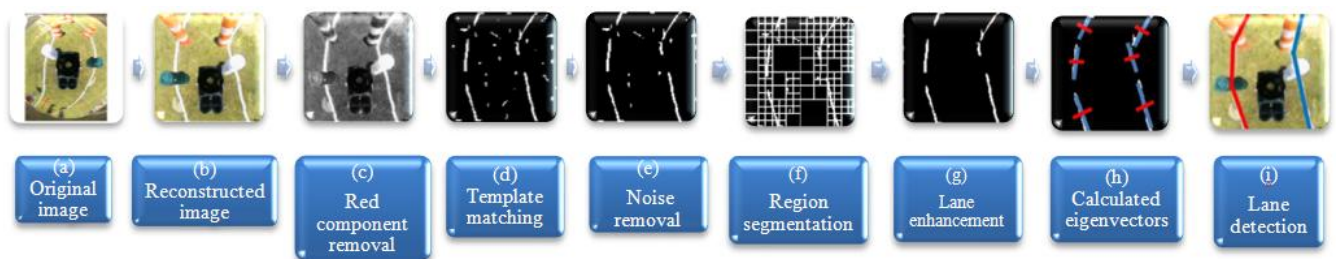

Figure 17 Lane detection

6.4 Path Planning

In Active2011, we employed an A*-search-based path planning algorithm to find the appropriate route. However, despite finding the shortest path with this algorithm, the vehicle could not track the path in the obstacle area during the autonomous challenge. To take into account the relation between obstacle positions while tracking the course, we introduced a potential field to generate an appropriate route without colliding with obstacles. According to the FMEA, we found that the A* search algorithm is one of the most time-consuming parts when finding the appropriate route. In order to reduce the processing time, a pruning algorithm is implemented in our A* search algorithm. Figure 18 (a) and (b) shows the difference between conventional and proposed path planning results. As shown in Figure 18 (b), the new path planning algorithm only generates half of the path, hence significantly reducing the search time.

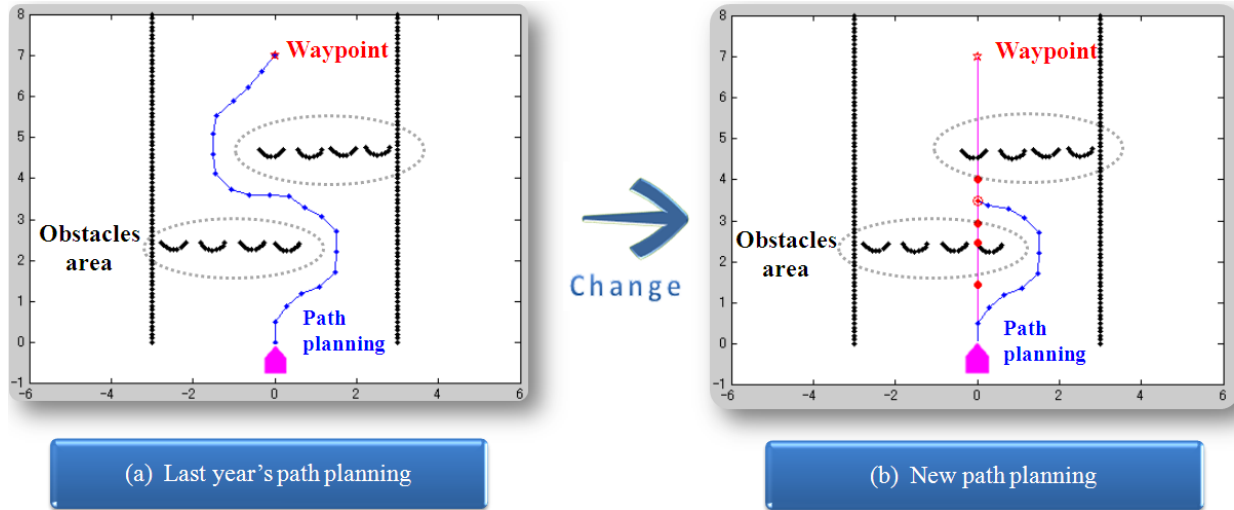(a) Last year's path planning   (b) New path planning

Figure 18 Simulated path planning

Table 9 shows processing time comparison between conventional algorithm and proposed algorithm. The proposed algorithm is improved about two times processing speed.

Table 9 Comparison difference between conventional and proposed algorithms

6.6 JAUS

In order to enhance the controllability and visibility of JAUS messages, we developed a new Android-based monitor that can be used as JAUS common operating picture (COP). The message command from COP was displayed on an Android tablet. It enables an easy configuration change even outdoors. Figure 19 shows the JAUS COP software for Android tablets. Excluding the COP, the remaining part is based on MATLAB and Python, the shared memory configuration being the same as last year. The JAUS control system that assumes the base receives the COP message

Figure 19 JAUS COP software for Android tablet

command from the laptop-PC through a wireless RF module data link. For the interpretation of the received command message, we use both MATLAB and Python. Because both are interpreted languages, verification and execution of the software can be done without recompilation. Communication between the two languages is done by using the shared memory.

7. Performance

Table 10 presents a comparison between the predicted parameters and the actual experimental results. The majority of predicted parameters are in agreement with the actual experimental results.

Table 10 Vehicle performance

Performance Measure	Performance Prediction	Performance Results
Maximum speed	4.1 mph (6.5 km/h)	3.5 mph (5.6 km)
Ramp climbing ability	10-degree incline	9.8-degree incline
Reaction times	0.3 seconds	0.4 to 0.5 seconds
Battery life	3 hours	2 hours
Obstacle detection distance	0 to 10 meters	0 to 10 meters
Waypoint accuracy	± 0.14 meters	± 0.14 meters

7.1 Speed

According to the original YAMAHA JW-Active specifications, the maximum speed is of 4.1 mph. However, because of the weight difference between the original wheelchair and our developed robot, we recorded a maximum speed of 3.5 mph during the actual experiments.

7.2 Climbing Ability

According to the original YAMAHA JW-Active catalog specifications, the expected climbing ability is about 10-degree incline. As in the previous case, the climbing ability of Active2012 is reduced up to 9.8-degree incline because of a 20% weight difference.

7.3 Reaction Time

It takes approximately 0.4 to 0.5 s to run the developed system algorithms. If an emergency stop occurs at 4.1 mph, which is the maximum speed, the vehicle will move about 0.5 meters before reacting.

7.4 Battery

A nickel metal hydride battery was used for the motor system and all the subsystems. This battery provides 24 Ah, allowing approximately 1 h of operating time. Additionally, the laptop-PC battery can operate for 5 h at full CPU load without feeding from the nickel battery.

7.5 Evaluation of Positioning Accuracy in Waypoint Navigation

The positioning accuracy of navigation waypoints was tested and evaluated.

The accuracy of Active2012's arrival at navigation waypoints is limited by the standard deviation of the D-GPS, which navigates with an error of less than ±0.14 m.

8. Conclusion

In this report, we presented the design and implementation of Active2012 and demonstrated its high safety, reliability, and durability. We described stepwise how software and hardware problems were overcome by using FMEA. Moreover, we constructed a robust and reliable robotic system by using a new 3D Scanner and Kinect. In order to reduce the processing time, we implemented a pruning algorithm in the A* search algorithm and employed eigenvector-based path planning. We achieved a significantly reduced search time. Active2012 has outstanding potential and we are confident that it will be a competitive force at the IGVC 2012.